

Investigation of the natural ventilation of wind catchers with different geometries in arid region houses

N. Sakhri^{1*}, Y. Menni², H. Ameur³, A. J. Chamkha⁴, N. Kaid³, M. Bensafi¹, G. Lorenzini⁵ and O. D. Makinde⁶

¹ Laboratory of Energy in Arid Areas (ENERGARID) University of Bechar, P.O. Box 417, 08000, Bechar, Algeria
Phone: +213-663368113

² Unit of Research on Materials and Renewable Energies, Department of Physics, Faculty of Sciences, Abou Bekr Belkaid University, P.O. Box 119, 13000, Tlemcen, Algeria

³ Department of Technology, University Centre of Naama - Salhi Ahmed, P.O. Box 66, Naama 45000, Algeria

⁴ Faculty of Engineering, Kuwait College of Science and Technology, 7th Ring Road, Doha, Kuwait

⁵ Department of Engineering and Architecture, University of Parma, Parco Area delle Scienze, 181/A, Parma 43124, Italy

⁶ Faculty of Military Science, Stellenbosch University, Private Bag X2, Saldanha 7395, South Africa

ABSTRACT – The wind catcher or wind tower is a natural ventilation technique that has been employed in the Middle East region and still until nowadays. The present paper aims to study the effect of the one-sided position of a wind catcher device against the ventilated space or building geometry and its natural ventilation performance. Four models based on the traditional design of a one-sided wind catcher are studied and compared. The study is achieved under the climatic conditions of the South-west of Algeria (arid region). The obtained results showed that the front and Takhtabush's models were able to create the maximum pressure difference (ΔP) between the windward and leeward of the tower-house system. Internal airflow velocities increased with the increase of wind speed in all studied models. For example, at $V_{wind} = 2$ m/s, the internal flow velocities were 1.7, 1.8, 1.3, and 2.5 m/s for model 1, 2, 3, and 4, respectively. However, at $V_{wind} = 6$ m/s, the internal flow velocities were 5.6, 5.5, 2.5, and 7 m/s for model 1, 2, 3, and 4, respectively. The higher internal airflow velocities are given by Takhtabush, traditional, front and middle tower models, respectively, with a reduction rate between the tower outlet and occupied space by 72, 42, 36, and 33% for the middle tower, Takhtabush, traditional tower, and the front model tower, respectively. This reduction is due to the due to internal flow resistance. The third part of the study investigates the effect of window (exist opening) position on the opposite wall. The upper, middle and lower window positions are studied and compared. The air stagnation or recirculation zone inside the ventilated space reduced from 55% with the lower window to 46% for the middle window and reached 35% for the upper window position. The Front and Takhtabush models for the one-sided wind catcher with an upper window position are highly recommended for the wind-driven natural ventilation in residential houses that are located in arid regions.

ARTICLE HISTORY

Revised: 10th Apr 2020

Accepted: 23rd Apr 2020

KEYWORDS

Natural ventilation;
wind driven;
wind catcher;
climatic conditions;
CFD

INTRODUCTION

Thermal Comfort

Thermal comfort was and still a significant concern, especially after the petrol crisis and fuel price rises. Occupied spaces must be conditioned and controlled. Forty percent of the total world energy consumption is used by the building sector, especially in office buildings that produce more carbon and greenhouse gas. In the USA and UK office buildings, more than 70% of energy is used only by lighting and ventilation [1]. HVAC (Heating, Ventilating and Air Conditioning) systems can be responsible for almost 68% of energy consumption in residential buildings [2]. The building ventilation can be provided naturally, mechanically, or by both sources called hybrid ventilation. The natural ventilation is defined as the natural air movement inside a structure without any contribution of fans or mechanical equipment. The two main types of the natural ventilation types the wind-driven and buoyancy-driven natural ventilation [3].

By experiments and numerical simulation, Mansor et al. [4] studied the effect of natural and artificial ventilation inside a car on the thermal comfort of passengers. They developed a numerical model to predict the reduction of internal car temperature by increasing the mass flow rate of ventilation. Other researchers studied the heat transfer efficiency [5-7]. In addition, Phase Change Materials (PCMs) technology is widely used in arid regions to enhance the occupant's thermal comfort [8-11]. For cooling applications, Dulaimi et al. [12] investigated the thermal performance of a natural draft wet cooling tower, natural draft condition, and a forced draft condition created by an axial fan. Their results showed a 22% increase in the cooling effectiveness in comparison with the traditional techniques. Zafirah and Mardiana [13] evaluated the performance of an air-to-air energy recovery system in terms of latent efficiency. They recovered energy to enhance the thermal comfort inside buildings under a hot and humid climate.

Natural Ventilation

Wind-driven ventilation occurs via pressure difference between the windward and leeward or between inlet and outlet openings in a ventilated space [14]. Buoyancy-driven ventilation occurs via the density difference between the warm and cold air existing in the same structure [15-25]. Warm air (less dense) leaves the ventilated space through upper openings, and it is replaced by the cold outside air (denser) via openings such as doors and windows. The solar chimney is an example of buoyancy-driven natural ventilation.

Natural ventilation appears as a sustainable solution for thermal comfort, health, and air quality improvement. A study on 12 public office buildings in Northern California touched 880 workers showed that the natural ventilation is more satisfactory with less sick building symptoms in comparison with the mechanical and HVAC ventilation [26].

Wind-Driven Natural Ventilation

The wind vertical profile in atmospheric boundary layer (ABL) follows a logarithmic power law:

$$\frac{u}{u_r} = \left(\frac{z}{z_r}\right)^\alpha \tag{1}$$

where u is the wind speed at z height, u_r is the reference of wind speed at a reference height z_r , α is an empirical parameter, the exponent (α) is an empirically derived coefficient that varies dependent upon the stability of the atmosphere (Figure 1). For neutral stability conditions, (α) is approximately 0.143 [27].

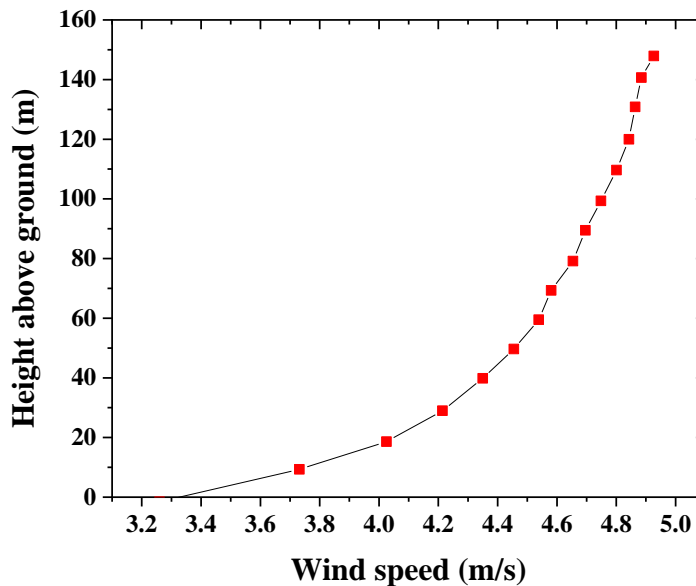


Figure 1. Vertical wind profile speed (for an open space, roughness class = 0.5, roughness length = 0.0024 m, $u_r = 3$ m/s, $z_r = 10$ m)

MATHEMATICAL MODELLING OF THE PROBLEM

Governing Equations

Liquids and gases circulating at low speeds behave like incompressible fluids [28, 29]. The governing equations for an incompressible fluid like atmospheric air in the rigorous sub-layer are written as follow:

Continuity equation:

$$\frac{\partial \bar{u}}{\partial x} + \frac{\partial \bar{v}}{\partial y} + \frac{\partial \bar{w}}{\partial z} = 0 \tag{2}$$

$$\frac{\partial u'}{\partial x} + \frac{\partial v'}{\partial y} + \frac{\partial w'}{\partial z} = 0 \tag{3}$$

$$\frac{\partial U}{\partial x} + \frac{\partial V}{\partial y} + \frac{\partial W}{\partial z} = 0 \tag{4}$$

where U, V, and W are the instantaneous speeds. \bar{u} , \bar{v} , \bar{w} are the average speeds. u' , v' , w' are the fluctuating speeds. Navier-Stokes equations are presented as follow:

$$\frac{\partial(\rho u)}{\partial t} + \frac{\partial(\rho uu)}{\partial x} + \frac{\partial(\rho vu)}{\partial y} + \frac{\partial(\rho wu)}{\partial z} = -\frac{\partial P}{\partial x} + \mu \left(\frac{\partial^2 u}{\partial x^2} + \frac{\partial^2 u}{\partial y^2} + \frac{\partial^2 u}{\partial z^2} \right) \tag{5}$$

$$\frac{\partial(\rho v)}{\partial t} + \frac{\partial(\rho uv)}{\partial x} + \frac{\partial(\rho vv)}{\partial y} + \frac{\partial(\rho wv)}{\partial z} = -\frac{\partial P}{\partial y} + \mu \left(\frac{\partial^2 v}{\partial x^2} + \frac{\partial^2 v}{\partial y^2} + \frac{\partial^2 v}{\partial z^2} \right) \tag{6}$$

$$\frac{\partial(\rho w)}{\partial t} + \frac{\partial(\rho uw)}{\partial x} + \frac{\partial(\rho vw)}{\partial y} + \frac{\partial(\rho ww)}{\partial z} = -\frac{\partial P}{\partial z} + \mu \left(\frac{\partial^2 w}{\partial x^2} + \frac{\partial^2 w}{\partial y^2} + \frac{\partial^2 w}{\partial z^2} \right) \tag{7}$$

The study of building natural ventilation is composed of two parts: envelope flows and internal air motion [30]. The envelope flows study the effect of wind on the ventilated space envelope that is also called the wind-structure interaction. Internal airflow studies the interior airflow characteristics (pressure, velocity, streamline, etc.). For the wind-driven natural ventilation, the external and internal pressure fields, as well as the internal airflow, must be identified.

The internal airflow velocity is one of the six basic parameters of thermal comfort. It plays a vital role in heat losses through the convection and evaporation for inhabitants inside a structure (a residential or an office building), enhancing thus the IAQ and providing suitable living conditions. As illustrated in Figure 2, The natural ventilation device must be well chosen and placed in a proper distribution of internal air to meet the standards of thermal comfort requirements.

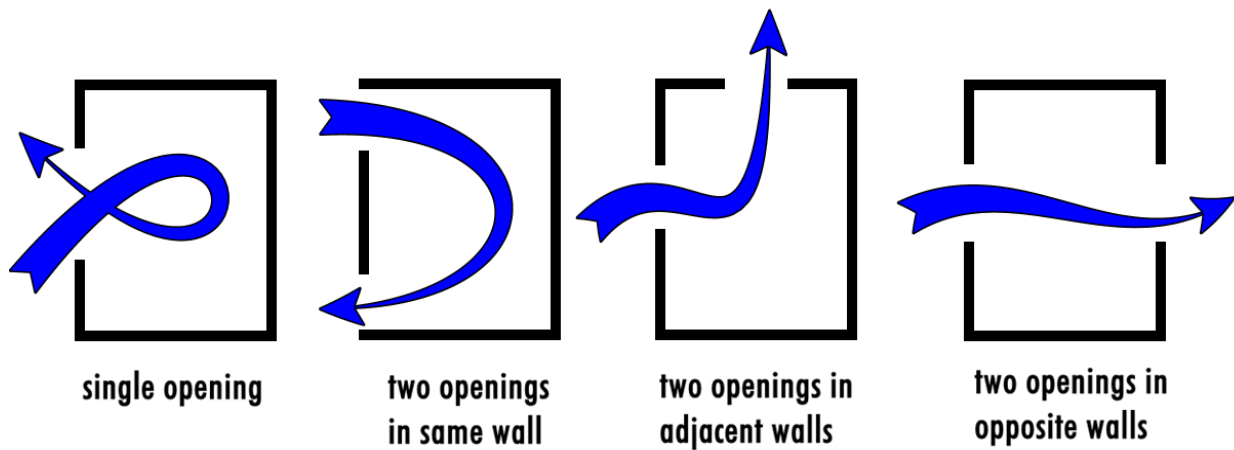


Figure 2. Types of the wind-driven natural ventilation

Wind Catchers Between Past, Present and Future

Wind catchers or BADGERS were used in the Middle-East region since old times. They have been known as an Iranian ventilation technique used in houses and mosques or related to the Qanat (an underground water system) [31], or to cool down the water in a reservoir and Yakhchal (an ice storage space) [32]. However, the wind catcher technique back to 1300 B.C in the Pharaonic times [33-36], as shown in Figure 3.

The traditional wind towers or catchers work in the presence and absence of wind by both pressure and buoyancy forces. In the presence of the wind, the device catches the prevailing winds. It redirects the airflow inside the building by using the pressure difference between the windward and leeward of (tower-structure) the system, and between the tower inlet and outlet, which is in the same time the air discharge opening. In the absence of the wind, the buoyancy forces are dominants, and the wind catcher works like a chimney. The night cooling is another advantage of wind catchers.

The modern wind catchers or mono-draught catch the wind near the building roof. They present the advantage of two- to four-sided wind catchers able to work 360° with various wind directions and angles. Nevertheless, the turbulence in the building roof level can decrease the ventilation performance by reducing the airflow rate entering the device (Figure 4).

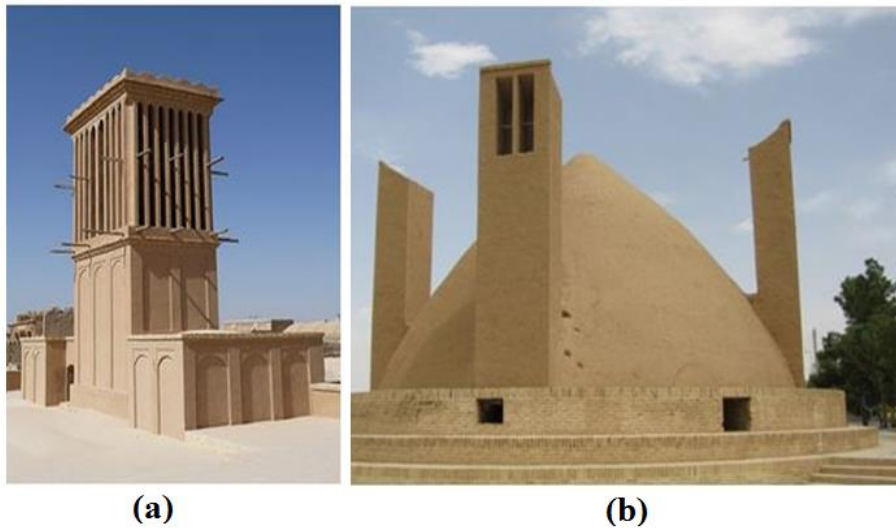


Figure 3. Yazd traditional wind-catcher for: (a) house ventilation and (b) water cooling

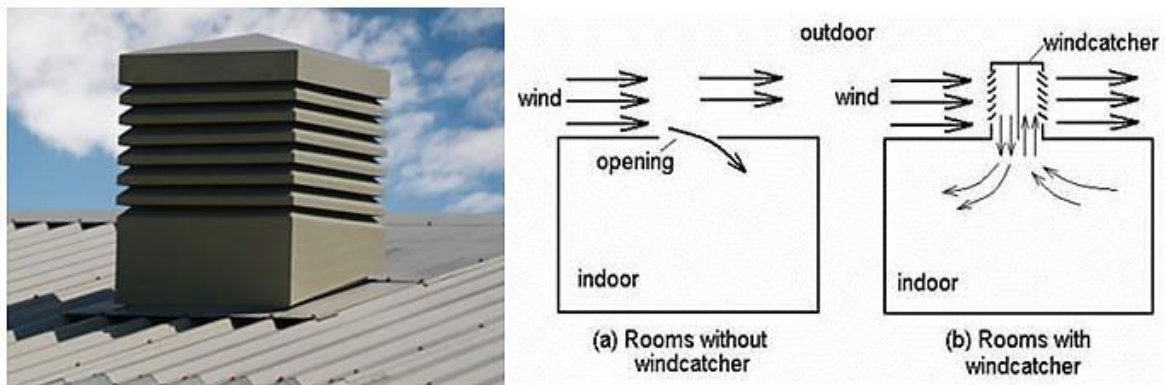


Figure 4. Schematic diagram of the modern wind catcher

The newly proposed models are based on a traditional design. The first model is a traditional Iranian wind catcher with an air-channel between the device and the ventilated space. This model is similar to the wind catchers that are used with water reservoirs. The second model is the Malqaf in Egyptian houses, as shown in Figure 5. Malqaf or Mulqaf is the Arabian name of wind catcher. A very good example of Malqaf use appears in Muhib Al-Din house (1350) in Cairo [37]. A natural ventilation system combines malqaf, dorq'ah (the central part of the structure) and the lantern in one structure to ensure a good circulation of fresh air in the qa'a (reception hall). Malqaf is placed in the windward side, facing the prevailing winds (Figure 6). It is generally made of wood or local materials with a 30° to 45° inclined roof in the opposite wall that is facing the prevailing winds [38].

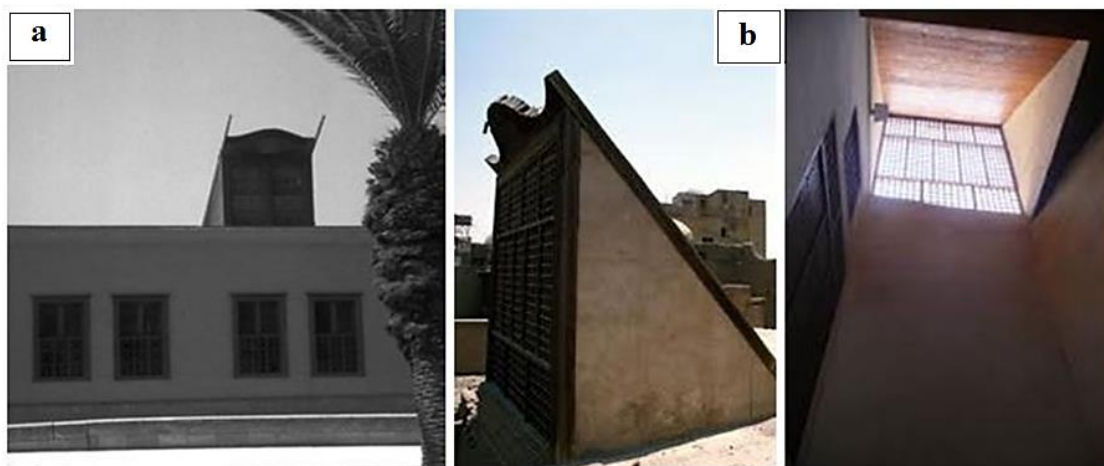


Figure 5. Malqaf at Al-Jawhara house in Cairo, Egypt with outside and inside view of the device

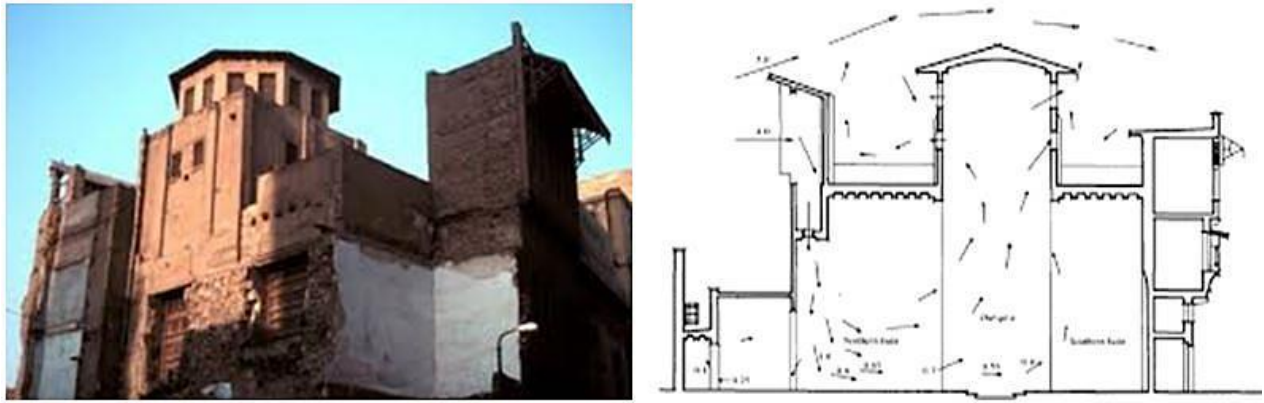


Figure 6. House of Muhib Ad-Din equipped with Malqaf, Cairo [33]

The third model is a one-sided wind catcher placed in the middle of the ventilated space roof to simulate the modern wind catcher. The fourth model is an old technique named Takhtabush (Figure 7a). Takhtabush is a covered outdoor sitting area located off the courtyard and in the nearest area to the entrance covered by a wooden grid called Musharabia [39, 40]. The new model is based on the geometry and position of Takhtabush (Figure 7b). It is placed in the windward side of the ventilated space, and the tower outlet is in the upper corner of the windward wall with an inclined base.



Figure 7. (a) Takhtabush in an old Egyptian house and (b) New model is based on the geometry and position of Takhtabush

NUMERICAL SIMULATION OF EXTERNAL AIRFLOWS AROUND A TOWER-HOUSE SYSTEM

Computational Wind Engineering (CWE) is a computational tool for wind-structure and natural ventilation studies. The outside domain or macroclimate is the atmospheric air considered as incompressible [41]. The macro domain dimensions (Figures 8 and 9) were chosen under the recommendation of [42, 43] to take into account the blockage ratio effect (equal to 16% in our case). The wind catcher height (H) is equal to 9 m.

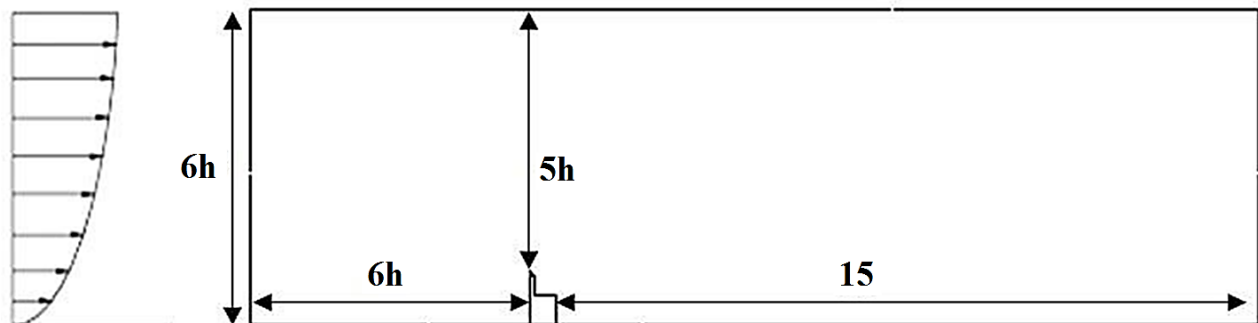


Figure 8. Dimensions of the Macroclimate or outside domain

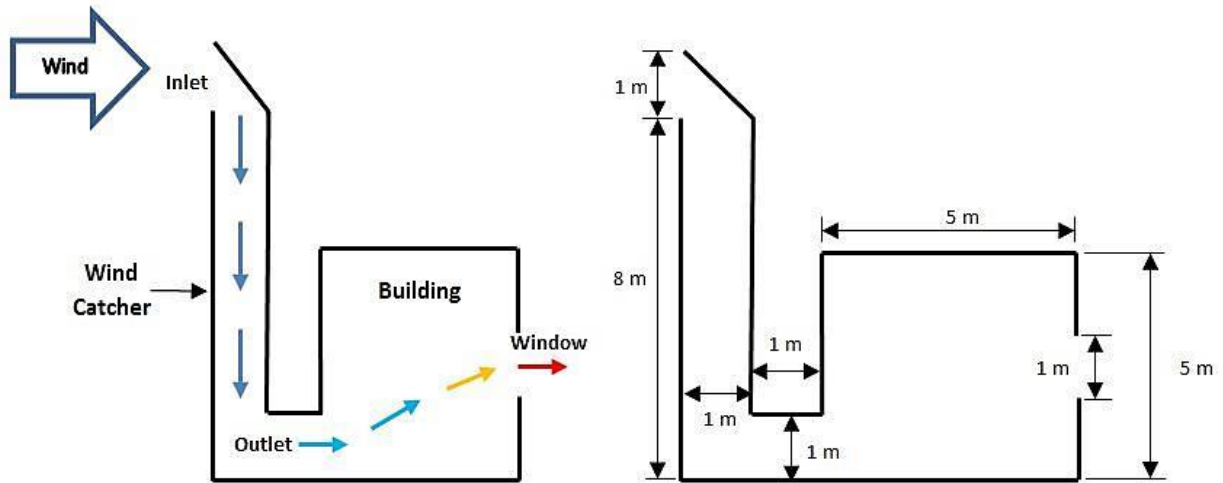


Figure 9. Tower-house schematic diagram and dimensions

Geometry and Dimension

For all studied models, the maximum value of H is equal to 9 m. The top and side views of the four models are presented. The cross-section of the wind catcher device and the air channel is 1 m² square shape. The inlet and outlet sections of the tower are equal to one m². Dimensions of the envelope of the ventilated space are chosen to simulate real room conditions, with L × H = 5 × 5 m² for the envelope. The surface of the window or air exit opening is equal to 1 m². An inclination by 45° in the roof catcher is chosen due to its aerodynamic efficiency and high airflow velocity, in comparison with the flat roof [44, 45] (Figure 10).

Grid and Mesh

To capture the details of the wind-structure interaction, a refined tetrahedral mesh is used starting from 10⁻³ m near the boundary layer of the tower-house system to 10⁻² m near the outside domain borders (Figure 11). Table 1 provides the grid details for each model.

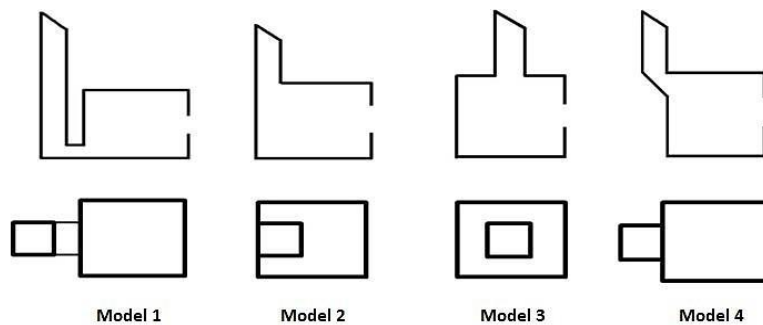


Figure 10. Side and top views of the four studied models

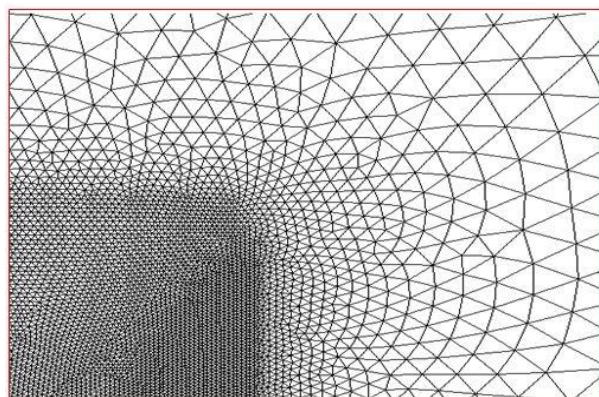


Figure 11. Tetrahedral refined mesh at the boundary layer of the tower-house system

Table 1. Grid information of the simulation cases

Model	Cells	Faces	Nodes
1	217 008	327 181	110 167
2	171 364	258 373	87 005
3	237 348	357 644	120 290
4	177 346	267 442	90 090

Boundary Conditions

The domain contains fully turbulent atmospheric air with a steady-state, and the house tower is considered as solid. Values of the velocity and pressure are set at the inlet and outlet sections, respectively. Symmetry and wall conditions are set for the upper border and domain base, respectively (Figure 12). The walls of the wind catcher and house are smooth. The $k-\epsilon$ model with pressure-based and standard wall function is used for the turbulence modeling. The SIMPLE method with the second-order upwind discretization scheme is used in this study due to its performance in CWE studies [46-51].

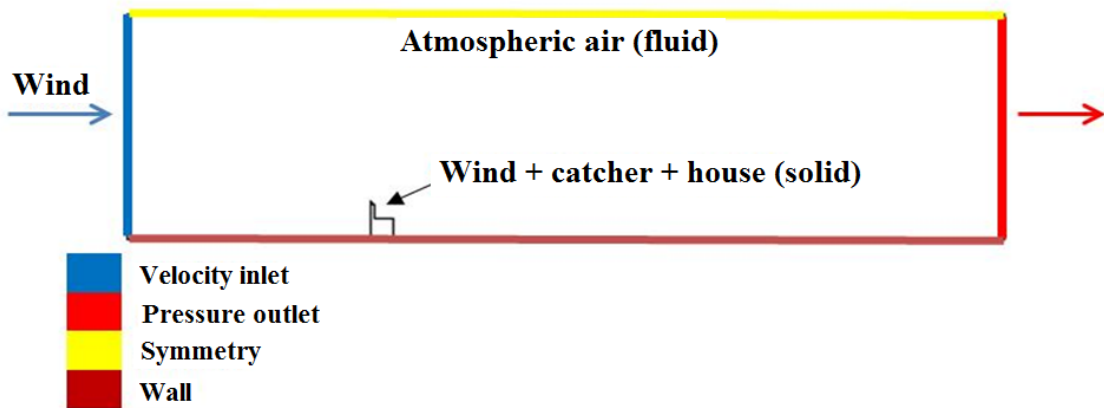


Figure 12. Boundary conditions for the external flow around a tower-house system

The south-west of Algeria was taken as a case study (Figure 13). It concerns an arid region characterized by the thermal discomfort, especially in the summer season. The mean wind speeds in this region are as follows: Béchar with 3.7 m/s, Adrar with 6.1 m/s, and Tindouf with 5.7 m/s [52]. The wind speed at domain inlet is 3 m/s (reference: Bechar region wind speed).

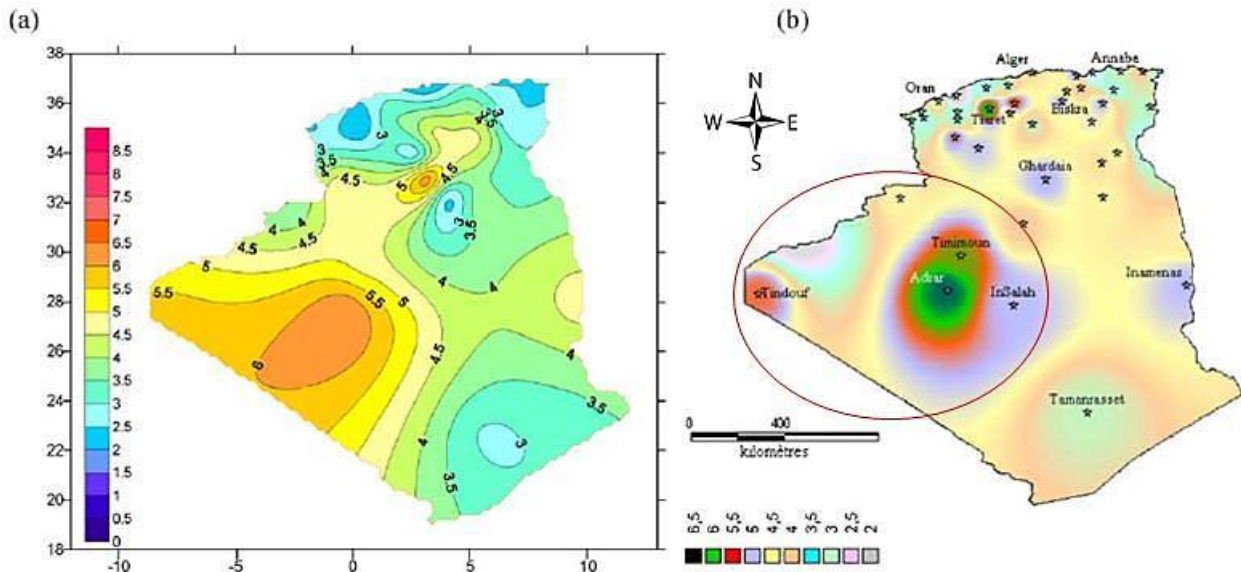


Figure 13. Algerian annual wind speed at 10 m of height

RESULTS AND DISCUSSION

The total pressure analysis of external envelope flows of a house equipped with a wind catcher device present a positive pressure on the windward side and a negative pressure on the leeward side for all models. The value 20.8 Pa of external pressure difference on the wind catcher was created in model 4 (Takhtabush), followed by 20.6 Pa for the traditional tower, 18.1 Pa for the front model tower, and 16 Pa for the middle tower (Table 2).

Table 2. External total pressure (Pa) and pressure coefficients of the models under investigation

Model	Wind-catcher				Room			
	Total pressure (Pa)		Pressure Coefficient		Total pressure (Pa)		Pressure Coefficient	
	Windward	Leeward	Windward	Leeward	Windward	Leeward	Windward	Leeward
Model 1 Traditional	13.1	-7.5	21	-12.5	-6	-8	-12.5	-12.5
Model 2 Front	11.4	-6.7	12.1	-12.4	13.3	-7.3	20.8	-12.4
Model 3 Middle	9	-7	11.2	-12.4	12.4	-7.4	19.6	-12.4
Model 4 Takhtabush	13.6	-7.2	14.4	-12.1	12.1	-7.2	21.5	-12.1

For the external pressure of the envelope, the maximum values of the created pressure difference were 20.6, 19.8, 19.3 Pa for models 2, 3, and 4, respectively. For the first model, (-2) Pa was the ΔP across the envelope equipped with a traditional wind catcher (Figure 14). This value was the result of the place of a traditional wind catcher, which acts as a protection or a shield. A negative pressure is created in both wind and leeward sides of the ventilated space and prevents the interaction between the wind and envelope windward side. Pressure coefficient is defined as:

$$C_p = (P - P_{ref}) / (0.5 \rho V_{ref}^2) \tag{8}$$

where P (Pa) is the local surface pressure, P_{ref} (Pa) and V_{ref} (m/s) are, respectively, the upstream static pressure and free stream velocity (wind), and ρ (kg/m³) is the air density. The values of the pressure coefficient on the wind catcher and envelope windward side of model 4 were higher than those of all studied models. The highest Cp conducts to the most efficient natural ventilation.

Analysis of the streamline in Figure 15 shows the existence of a recirculation zone in the leeward side of the wind catcher device in all studied models. An additional recirculation zone exists in the middle wind catcher, which can reduce the airflow at the inlet of the device. A small recirculation zone is created above the air channel that connects the traditional wind catcher and the envelope, resulting thus an additional negative pressure in the windward of the envelope as well as in the ventilated spaces.

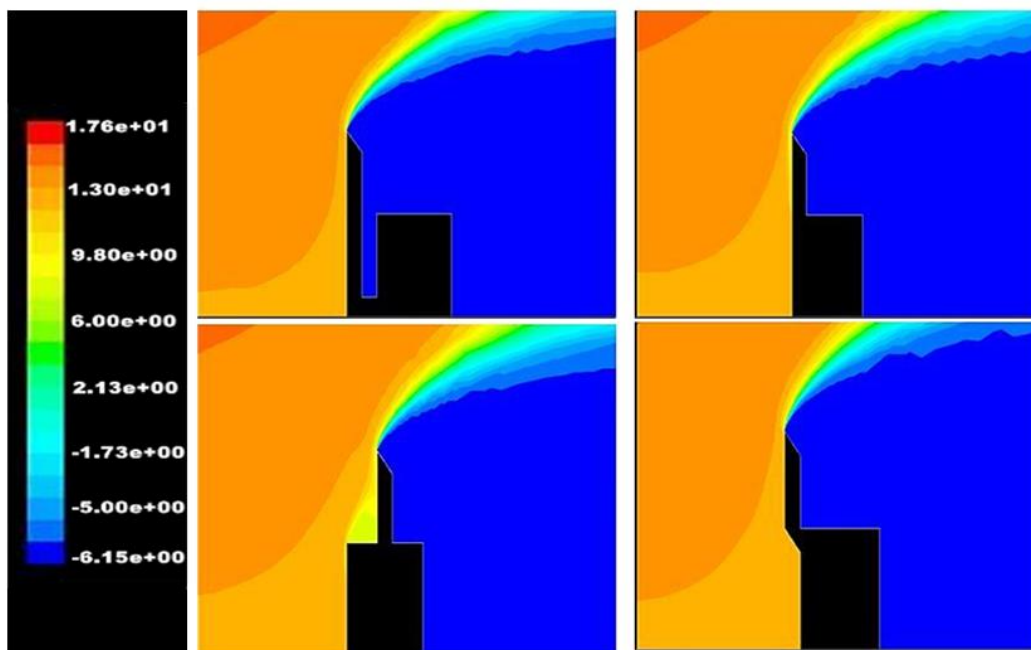


Figure 14. Total external pressure (Pa) with V_{wind} = 3 m/s

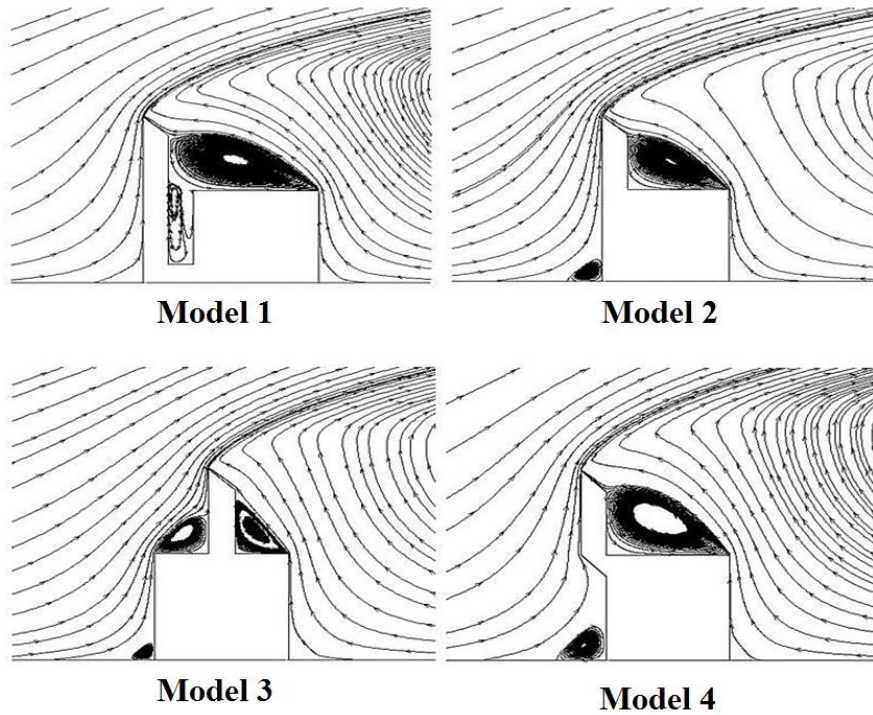


Figure 15. External streamline of airflow around the structures (tower and house)

Analysis of the Internal Airflow in Ventilated Spaces

The airflow inside the ventilated area is widely influenced by the external airflow around it. The thermal comfort in building occupants is directly related to the internal pressure and airflow velocity. The following values of wind speed, namely: 1, 2, 3, 5, 6, and 10 m/s, are chosen based on the weather conditions of the region (south-west of Algeria). For further details, the envelope was divided into nine equal sub-zones as illustrated in Figure 16. The total internal pressure and airflow velocities are discussed. The analysis of the internal pressure has given the following results:

High pressure was observed in front and Takhtabush models in five zones: A, C, D, F, and G. The most elevated total pressure of 37 Pa existed in the Takhtabush model, especially in the G zone. As observed in Figure 17, the highest values of pressure were located in G, H, and I zones due to the air density and internal airflow. For the middle tower model, the highest value of total pressure exists in zone B due to the discharge opening. However, the lowest value is observed in zone C, which presents a dead fluid or a stagnation zone where the airflow is recirculated.

The middle tower model offers the lowest values of total pressure among all models, because of the existence of a short loop of airflow between the discharge orifice and window (Figure 18).

A	B	C
D	E	F
G	H	I

Figure 16. Envelope space divided in 9 sub-zones

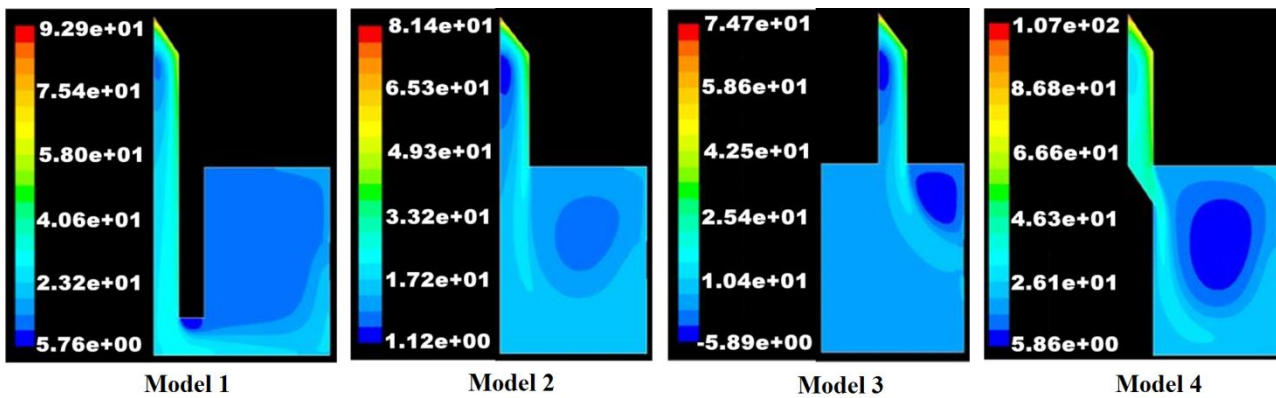


Figure 17. Total internal pressure (Pa) with $V_{wind} = 3$ m/s

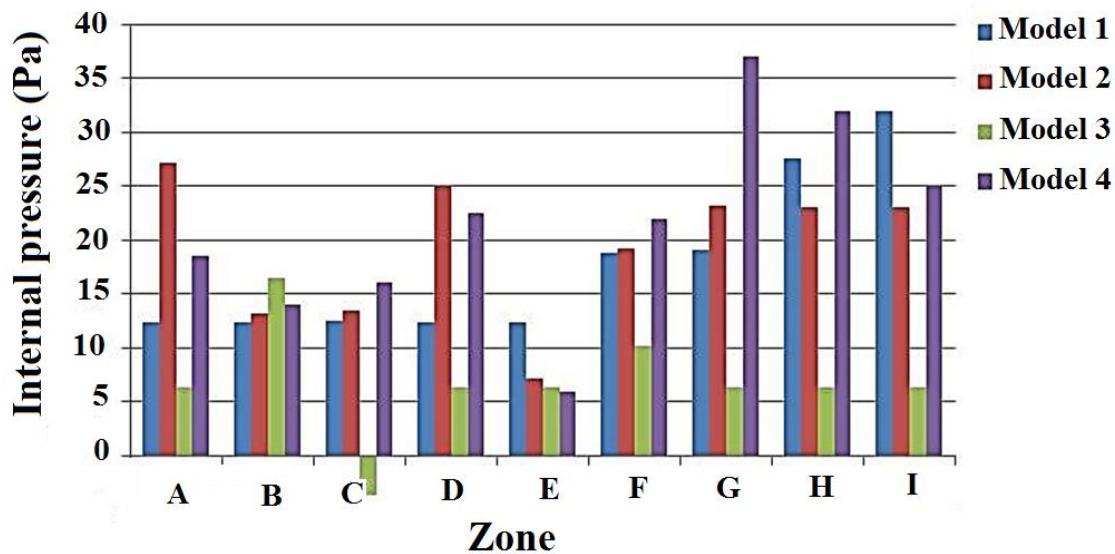


Figure 18. Internal total pressure (Pa) for the four studied models with $V_{wind} = 3$ m/s

The traditional wind tower with A, B, C zones and the middle tower with D and E zones present a uniform pressure zones, and the high values exist in G, H, and I zones. The high pressure in these zones is the result of discharge or injection orifice from the catcher outlet to the ventilated space. Air pressures in zone F are probably the same (between 18 and 22 Pa) in all models. This is due to the existence of the window, where the airflow leaves the envelope.

For the velocity magnitude, the highest values were observed at the discharge opening (or the tower outlet that is connected directly with the envelope). These maximum values were 4.9, 4.5, 4.4, and 4.2 m/s for Takhtabush, front model in zone A, middle tower at zone C, and traditional wind catcher at zone G, respectively. The lowest velocities characterize zone E, and the central recirculation zone is located at the center region of the space, which can cause a flow stagnation area (Figure 19 and Table 3). Airflow velocities in zone F are very close, and they vary between 3.85 and 3.36 m/s. These values present the outflow velocities of the internal air leaving the ventilated space.

The occupants of the ventilated space or the house occupied half of the area as showed in Figure 20, with H_{house} presents $\frac{1}{2} H_{house}$ equal to 2.5 m. For a wind speed varying between 1 and 10 m/s, the obtained figures give an idea about the internal airflow velocity from the tower outlet (air discharge orifice) through the occupied area until leaving the envelope by the window (exist opening). The obtained results in Table 4 show that the internal airflow velocities increase with the rise of wind speeds for all models.

Internal airflow velocity is reduced from the air discharge orifice to the occupied area by 33, 72, 42, and 36% for the front tower, middle tower, Takhtabush tower, and traditional wind catcher models, respectively. This velocity increases after leaving this area to the window opening for all four models. A sharp edge at the outlet of the Takhtabush tower model yields a high air velocity in comparison with the other studied models. The lowest airflow velocities in the occupied space occur in the middle tower model and very satisfactory results are reached for the three other models.

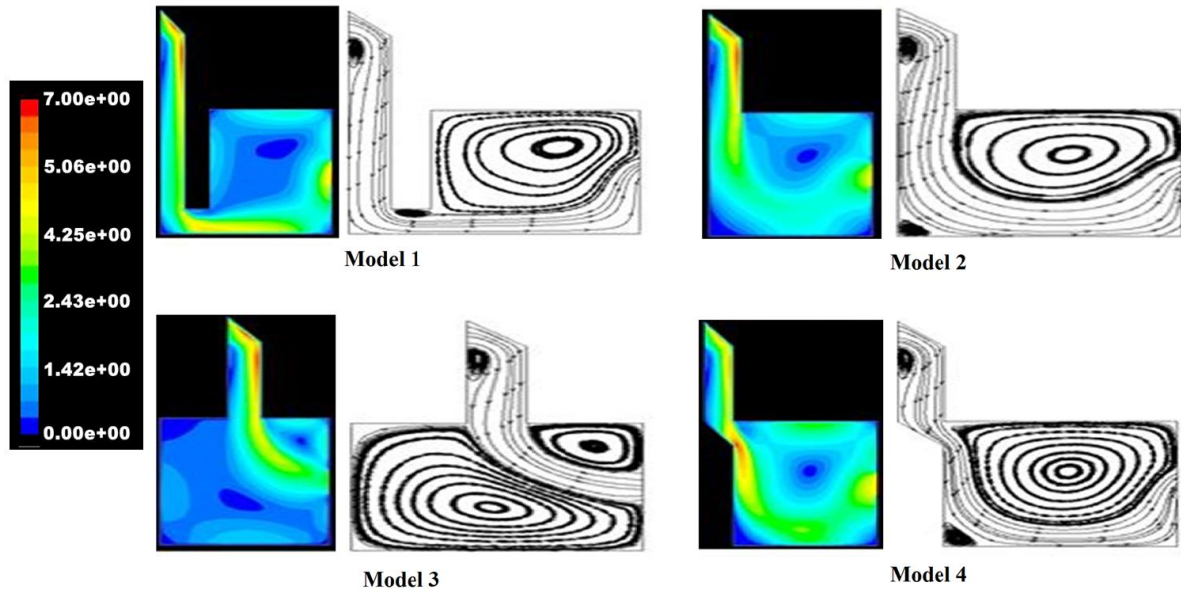


Figure 19. Internal airflow velocities and streamlines for the four studied models with $V_{wind} = 3\text{m/s}$

Table 3. Velocity magnitude of the internal airflow (m/s) for the four studied models, with $V_{wind} = 3\text{ m/s}$

Zone	A	B	C	D	E	F	G	H	I
Model 1	0.992	1.007	1.398	0.676	0.315	3.323	4.225	3.834	2.421
Model 2	4.466	0.631	1.007	3.263	0.977	3.443	1.187	2.631	1.729
Model 3	0.285	4.375	0.345	0.646	1.368	3.639	0.842	1.118	0.766
Model 4	4.842	3.187	1.909	4.241	0.646	3.789	3.739	3.624	2.842

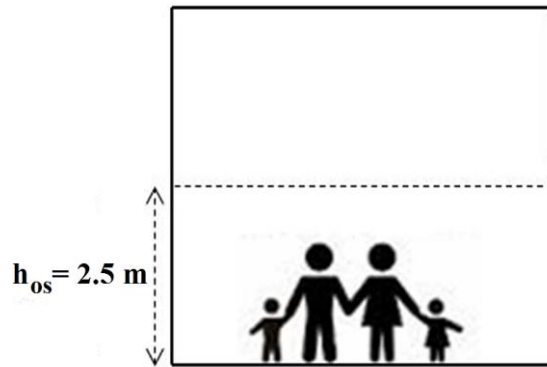


Figure 20. Occupied area by inhabitants

Table 4. Airflow velocities (m/s) inside the ventilated space with different wind speeds: $V_{wind} = 1, 2, 3, 5, 6$ and 10 m/s

	V_{wind} (m/s)	1	2	3	5	6	10
Model 1	Tower outlet	1.05	2.88	3.65	5.96	7.7	14.43
	Occupied space	0.48	1.25	2.41	4.33	5.01	9.43
	Window	1.05	2.98	4.13	7.41	9.62	16.74
Model 2	Tower outlet	1.05	2.20	3.35	5.45	7.18	12.63
	Occupied space	0.48	1.34	1.91	4.11	4.88	8.90
	Window	0.57	2.77	3.82	7.65	9.67	16.56
Model 3	Tower outlet	1.17	2.21	3.46	5.82	7.36	12.61
	Occupied space	0.14	0.73	0.95	2.28	4.05	3.97
	Window	1.17	2.28	3.16	5.01	6.11	10.75

Model 4	Tower outlet	1.70	3.50	4.89	10.10	11.27	18.51
	Occupied space	0.74	2.12	3.19	5.31	6.59	10.95
	Window	0.63	2.44	5.42	8.19	9.46	18.93

Effect of the Opening Position on Internal Airflow

The third part of the study is dedicated to the outflow opening or window position, as shown in Figures 21 and 22. Two additional locations are studied and compared with the usual window position that is generally located in the middle of the opposite wall of the structure. An upper window is located directly under the roof, and a lower position window is located directly above the envelope base. The front wind catcher was selected as a natural ventilation device.

The distribution of the total air pressure shows a uniform pressure field in the upper window model, compared with the middle and lower windows by a difference of 23 Pa. The same result was obtained for the airflow velocity magnitude with 2.65 m/s, which can reduce the internal temperature of the ventilated space by 4 to 5 °C [53].

The streamline analysis of the three configurations was compared in Figure 23. The size of the airflow stagnation zone of the occupied space equipped with a front tower model was 55, 46, and 35% for the lower window (case A), middle window (case B), and upper window (case C), respectively. The upper window or opening configuration is the most appropriate to reduce the central recirculation area and provide more airflows for the ventilated space occupants. Furthermore, the stagnation area is reduced with the increased height of the window position.

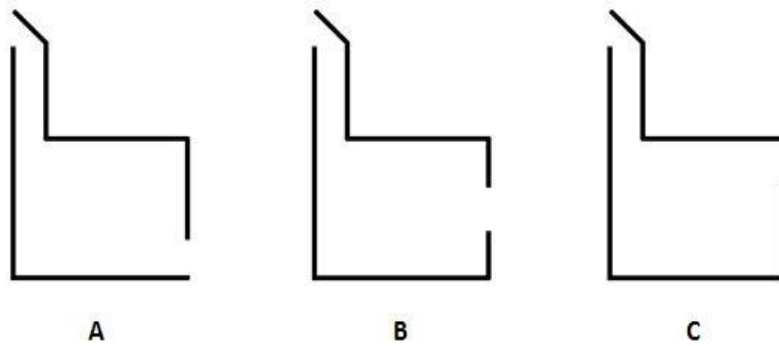


Figure 21. Tower-house system with different window positions

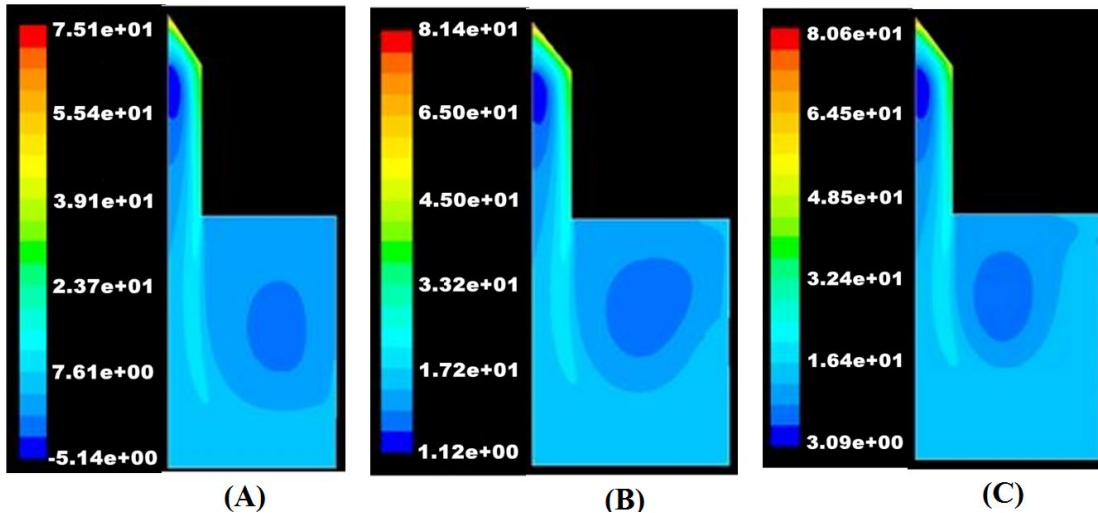


Figure 22. Internal total pressure (Pa) for three window positions: (a) down, (b) middle and (c) top ($V_{wind} = 3$ m/s)

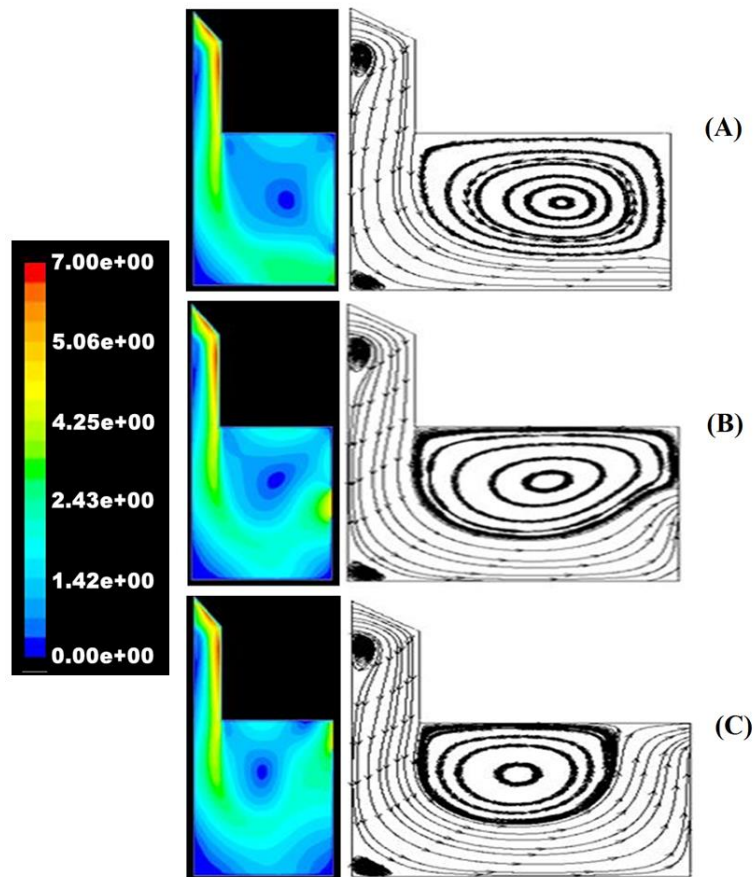


Figure 23. Internal airflow velocity (m/s) and streamlines for three window positions: (a) down, (b) middle, (c) top ($V_{\text{wind}} = 3 \text{ m/s}$)

CONCLUSION

The natural ventilation is taking more and more important in designing bioclimatic buildings due to thermal efficiency and cost-saving advantages. Naturally ventilated buildings must be well studied and dimensioned. Besides, the natural ventilation strategy and device choices must take into consideration the weather conditions of the region. Wind catchers have been employed for a very long time to nowadays because of their efficiency and variety of use (with Qanat, Yakhchal, solar chimney, courtyard, etc.). It is a technology that never stops development.

The performance of four one-sided wind catchers was studied to demonstrate the influence of the device position on natural ventilation. These models were: the Iranian traditional wind catcher, Mulkaif, modern wind catchers placed in the middle of the ventilated space. The last model was inspired from the Egyptian technique Takhtabush. The obtained results showed the importance of the device position on the system performance. The external airflow around the tower-house system indicated that front and Takhtabush models create the maximum pressure difference ΔP and pressure coefficient C_p between the windward and leeward of the system, compared to the traditional and middle towers, which lead to the best wind-driven natural ventilation. The second part of the study was a comparison of internal airflow proprieties inside the ventilated envelope equipped with the four studied models. The wind speed varied between 1, 2, 3, 5, 6, and 10 m/s based on the weather conditions of the South-West of Algeria (Bechar, Tindouf, Adrar). The results analysis has given the following conclusions:

- 1) The airflow velocities inside the building increased with the increase of wind speed in all models.
- 2) Front and Takhtabush models were able to create more airflow inside the ventilated space, in comparison with the middle and traditional catchers.
- 3) A reduction of internal airflow velocities from the tower outlet to the occupied space occupants by 72, 42, 36, and 33% was observed for the middle tower, Takhtabush tower, traditional tower, and front model, respectively.
- 4) The positions of Front and Takhtabush models against the ventilated space geometry are highly recommended in comparison with the middle tower position. The results of the traditional wind catcher are also very satisfactory.

- 5) The third part of the study clarified the effect of window position in the opposite wall on internal airflow stagnation or air recirculation area, and therefore on the wind-driven natural ventilation. The upper window was able to reduce the stagnation area by 20 and 11%, compared with the lower and middle window positions, respectively. The use of the upper window with the wind catcher technique allows the best natural ventilation by decreasing the stagnation zone, which also improves the IAQ inside the ventilated space. The wind catcher is a very promising technique for the wind-driven natural ventilation in residential houses that are located in windy and arid regions like the South-west of Algeria.
- 6) For future works, the authors will study by experiments the effects of the new models in arid regions.

ACKNOWLEDGMENTS

The authors are grateful to Mr. Nairi Abdelkarim for providing the site for the study.

REFERENCES

- [1] C. Siew, A. Che-Ani, N. Tawil, N. Abdullah, and M. Mohd-Tahir, "Classification of natural ventilation strategies in optimizing energy consumption in Malaysian office buildings," *Procedia Engineering*, vol. 20, pp. 363-371, 2011.
- [2] G. Evola and V. Popov, "Computational analysis of wind driven natural ventilation in buildings," *Energy and Buildings*, vol. 38, pp. 491-501, 2006.
- [3] E. H. Moghaddam, S. Amindeldar, and A. Besharatizadeh, "New approach to natural ventilation in public buildings inspired by Iranian's traditional windcatcher," *Procedia Engineering*, vol. 21, pp. 42-52, 2011.
- [4] M. Mansor, U. Rahman, M. Z. Abidin, M. M. Zain, and M. M. Yusof, "Variation of car cabin temperature influenced by ventilation under direct sun exposure," *Journal of Mechanical Engineering and Sciences*, vol. 6, pp. 1014-1023, 2014.
- [5] M. Nawi, A. Mamat, and H. Ismail, "Numerical heat transfer analysis of waste heat exchanger for exhaust gas energy recovery," *Journal of Mechanical Engineering and Sciences*, vol. 8, pp. 1498-506, 2015.
- [6] M. Ashham, S. Raheemah, and K. Salman, "Numerical investigation on enhancement of heat transfer using rod inserts in single pipe heat exchanger," *Journal of Mechanical Engineering and Sciences*, vol. 13, pp. 6112-6124, 2019.
- [7] D. Sahel, H. Ameer, and M. Mellal, "Effect of tube shape on the performance of a fin and tube heat exchanger," *Journal of Mechanical Engineering and Sciences*, vol. 14, pp. 6709-6718, 2020.
- [8] A. Hajjar, S. Mehryan, and M. Ghalambaz, "Time periodic natural convection heat transfer in a nano-encapsulated phase-change suspension," *International Journal of Mechanical Sciences*, vol. 166, p. 105243, 2020.
- [9] M. Ghalambaz, S. Mehryan, A. Hajjar, and A. Veismoradi, "Unsteady natural convection flow of a suspension comprising Nano-Encapsulated Phase Change Materials (NEPCMs) in a porous medium," *Advanced Powder Technology*, vol. 31, pp. 954-966, 2020.
- [10] M. Ghalambaz, T. Groşan, and I. Pop, "Mixed convection boundary layer flow and heat transfer over a vertical plate embedded in a porous medium filled with a suspension of nano-encapsulated phase change materials," *Journal of Molecular Liquids*, vol. 293, p. 111432, 2019.
- [11] M. Ghalambaz, A. J. Chamkha, and D. Wen, "Natural convective flow and heat transfer of nano-encapsulated phase change materials (NEPCMs) in a cavity," *International journal of heat and mass transfer*, vol. 138, pp. 738-749, 2019.
- [12] M. J. Al-Dulaimi, F. A. Kareem, and F. A. Hamad, "Evaluation of thermal performance for natural and forced draft wet cooling tower," *Journal of Mechanical Engineering and Sciences*, vol. 13, pp. 6007-6021, 2019.
- [13] M. Zafirah and A. Mardiana, "Experimental investigation on the performance of an air-to-air energy recovery for building applications in hot-humid climate," *Journal of Mechanical Engineering and Sciences*, vol. 10, pp. 1857-1864, 2016.
- [14] N. Sakhri, Y. Menni, and H. Ameer, "Experimental investigation of the performance of earth-to-air heat exchangers in arid environments," *Journal of Arid Environments*, vol. 180, p. 104215, 2020.
- [15] L. Kolsi, A. Abidi, M. Borjini, N. Daous, and H. Ben Aïssia, "Effect of an external magnetic field on the 3-D unsteady natural convection in a cubical enclosure," *Numerical Heat Transfer, Part A: Applications*, vol. 51, pp. 1003-1021, 2007.
- [16] L. Kolsi, H. F. Oztop, A. Alghamdi, N. Abu-Hamdeh, M. N. Borjini, and H. B. Aïssia, "A computational work on a three dimensional analysis of natural convection and entropy generation in nanofluid filled enclosures with triangular solid insert at the corners," *Journal of Molecular Liquids*, vol. 218, pp. 260-274, 2016.
- [17] M. N. Borjini, L. Kolsi, N. Daous, and H. B. Aïssia, "Hydromagnetic double-diffusive laminar natural convection in a radiatively participating fluid," *Numerical Heat Transfer, Part A: Applications*, vol. 48, pp. 483-506, 2005.
- [18] L. Kolsi, K. Kalidasan, A. Alghamdi, M. N. Borjini, and P. R. Kanna, "Natural convection and entropy generation in a cubical cavity with twin adiabatic blocks filled by aluminum oxide–water nanofluid," *Numerical Heat Transfer, Part A: Applications*, vol. 70, pp. 242-259, 2016.
- [19] A. Abidi, L. Kolsi, M. N. Borjini, and H. B. Aïssia, "Effect of radiative heat transfer on three-dimensional double diffusive natural convection," *Numerical Heat Transfer, Part A: Applications*, vol. 60, pp. 785-809, 2011.

- [20] C. Maatki, L. Kolsi, H. F. Oztop, A. Chamkha, M. N. Borjini, H. B. Aissia, and K. Al-Salem, "Effects of magnetic field on 3D double diffusive convection in a cubic cavity filled with a binary mixture," *International Communications in Heat and Mass Transfer*, vol. 49, pp. 86-95, 2013.
- [21] S. M. H. Zadeh, S. Mehryan, E. Izadpanahi, and M. Ghalambaz, "Impacts of the flexibility of a thin heater plate on the natural convection heat transfer," *International Journal of Thermal Sciences*, vol. 145, p. 106001, 2019.
- [22] S. Mehryan, M. Ghalambaz, R. K. Feeoj, A. Hajjar, and M. Izadi, "Free convection in a trapezoidal enclosure divided by a flexible partition," *International journal of heat and mass transfer*, vol. 149, p. 119186, 2020.
- [23] S. Mehryan, E. Izadpanahi, M. Ghalambaz, and A. Chamkha, "Mixed convection flow caused by an oscillating cylinder in a square cavity filled with Cu–Al 2 O 3/water hybrid nanofluid," *Journal of Thermal Analysis and Calorimetry*, vol. 137, pp. 965-982, 2019.
- [24] E. Jamesahar, M. Sabour, M. Shahabadi, S. Mehryan, and M. Ghalambaz, "Mixed convection heat transfer by nanofluids in a cavity with two oscillating flexible fins: A fluid–structure interaction approach," *Applied Mathematical Modelling*, vol. 82, pp. 72-90, 2020.
- [25] A. Alsabery, F. Selimefendigil, I. Hashim, A. Chamkha, and M. Ghalambaz, "Fluid-structure interaction analysis of entropy generation and mixed convection inside a cavity with flexible right wall and heated rotating cylinder," *International journal of heat and mass transfer*, vol. 140, pp. 331-345, 2019.
- [26] M. J. Mendell, W. J. Fisk, J. A. Deddens, W. G. Seavey, A. H. Smith, D. F. Smith, A. T. Hodgson, J. M. Daisey, and L. R. Goldman, "Elevated symptom prevalence associated with ventilation type in office buildings," *Epidemiology*, pp. 583-589, 1996.
- [27] G. Gualtieri, "Development and application of an integrated wind resource assessment tool for wind farm planning," *International Journal of Renewable Energy Research (IJRER)*, vol. 2, pp. 674-685, 2012.
- [28] N. Sakhri, Y. Menni, A. Chamkha, M. Salmi, and H. Ameer, "Earth to air heat exchanger and its applications in arid regions—an updated review," *TECNICA ITALIANA Ital J Eng Sci*, vol. 64, pp. 83-90, 2020.
- [29] J. Seifert, Y. Li, J. Axley, and M. Rösler, "Calculation of wind-driven cross ventilation in buildings with large openings," *Journal of Wind Engineering and Industrial Aerodynamics*, vol. 94, pp. 925-947, 2006.
- [30] D. Etheridge, "A perspective on fifty years of natural ventilation research," *Building and Environment*, vol. 91, pp. 51-60, 2015.
- [31] B. R. Hughes, J. K. Calautit, and S. A. Ghani, "The development of commercial wind towers for natural ventilation: A review," *Applied energy*, vol. 92, pp. 606-627, 2012.
- [32] G. Soltani, A. Nazari, and N. Ghanavati, "Energy Management in Iranian Maintainable Ancient Architecture" Introducing Ice Houses and Cisterns in Yazd City," *Canadian Journal on Environmental, Construction and Civil Engineering*, vol. 3, pp. 173-178, 2012.
- [33] A.-m. El-Shorbagy, "Design with nature: windcatcher as a paradigm of natural ventilation device in buildings," *International Journal of Civil & Environmental Engineering IJCEE-IJENS*, vol. 10, pp. 26-31, 2010.
- [34] H. Okhovat, N. Almasifar, and M. Reza Bemanian, "A research on historical and cultural buildings in iranian vernacular architecture," *ACE: architecture, city and environment*, vol. 6, pp. 37-58, 2011.
- [35] M. Dehghani-Sani, "Wind Towers: Architecture, Climate and Sustainability," ed: Taylor & Francis, 2018.
- [36] A. Mostafaeipour, B. Bardel, K. Mohammadi, A. Sedaghat, and Y. Dinpashoh, "Economic evaluation for cooling and ventilation of medicine storage warehouses utilizing wind catchers," *Renewable and Sustainable Energy Reviews*, vol. 38, pp. 12-19, 2014.
- [37] J. K. Calautit, B. R. Hughes, and S. S. Shahzad, "CFD and wind tunnel study of the performance of a uni-directional wind catcher with heat transfer devices," *Renewable Energy*, vol. 83, pp. 85-99, 2015.
- [38] S. Suleiman and B. Himmo, "Direct comfort ventilation. Wisdom of the past and technology of the future (wind-catcher)," *Sustainable Cities and Society*, vol. 5, pp. 8-15, 2012.
- [39] A. M. Salama, "A typological perspective: the impact of cultural paradigmatic shifts on the evolution of courtyard houses in Cairo," *METU Journal of the Faculty of Architecture*, vol. 23, pp. 41-58, 2006.
- [40] A. Petersen, *Dictionary of Islamic architecture*: Psychology Press, 1996.
- [41] T. Yang, "CFD and field testing of a naturally ventilated full-scale building," University of Nottingham, 2004.
- [42] J. Revuz, "Numerical simulation of the wind flow around a tall building and its dynamic response to wind excitation," University of Nottingham, 2011.
- [43] Y. Tominaga and T. Stathopoulos, "CFD simulation of near-field pollutant dispersion in the urban environment: A review of current modeling techniques," *Atmospheric Environment*, vol. 79, pp. 716-730, 2013.
- [44] H. Montazeri and R. Azizian, "Experimental study on natural ventilation performance of one-sided wind catcher," *Building and Environment*, vol. 43, pp. 2193-2202, 2008.
- [45] A. Dehghan, M. K. Esfeh, and M. D. Manshadi, "Natural ventilation characteristics of one-sided wind catchers: experimental and analytical evaluation," *Energy and Buildings*, vol. 61, pp. 366-377, 2013.
- [46] Y. Gao and W. Chow, "Numerical studies on air flow around a cube," *Journal of Wind Engineering and Industrial Aerodynamics*, vol. 93, pp. 115-135, 2005.
- [47] M. H. Ghadiri, M. F. Mohamed, and N. L. N. Ibrahim, "Cfd analysis of natural ventilation behaviour in four sided wind catcher," in *Proceedings of World Academy of Science, Engineering and Technology*, 2012, p. 704.

- [48] A. R. Vempati, "Computational Fluid Dynamics Investigation of Air Velocity and Temperature Distribution in a Room Equipped with Active Chilled Beam Air-conditioning," University of Florida, 2011.
- [49] S. Murakami, "Current status and future trends in computational wind engineering," *Journal of Wind Engineering and Industrial Aerodynamics*, vol. 67, pp. 3-34, 1997.
- [50] C. M. Mak, "Application of computational fluid dynamics to the study of designed green features for sustainable buildings," *Computational Fluid Dynamics*, p. 173, 2010.
- [51] A. A. Elmualim, "Effect of damper and heat source on wind catcher natural ventilation performance," *Energy and Buildings*, vol. 38, pp. 939-948, 2006.
- [52] F. Chellali, A. Khellaf, A. Belouchrani, and A. Recioui, "A contribution in the actualization of wind map of Algeria," *Renewable and Sustainable Energy Reviews*, vol. 15, pp. 993-1002, 2011.
- [53] R. Vittone, *Bâtir: manuel de la construction*: PPUR Presses polytechniques, 2010.